Supramolecular Chemistry

DOI: 10.1002/ange.201407555

# Supramolecular Assembly through Interactions between Molecular Dipoles and Alkali Metal Ions**

*Tomoko K. Shimizu, Jaehoon Jung, Hiroshi Imada, and Yousoo Kim**

***Abstract:*** *Establishing a way to fabricate well-ordered molecular structures is a necessary step toward advancement in organic optoelectronic devices. Here, we propose to use interactions between electric dipoles of molecules and alkali metal ions to form a well-developed homogeneous monolayer of diarylethene molecules on the Cu(111) surface with the aid of NaCl co-deposition. Scanning tunneling microscopy and density functional theory calculation results indicate that the formation of a row-type structure occurs as a result of interactions between the $Na^+$ ions and the diarylethene molecular dipoles, drastically changing the adsorption configuration from that without $Na^+$.*

A fundamental understanding of geometric structures and charge density distributions of molecules facilitates the prediction of interaction between molecules. It thus helps the design and fabrication of structurally homogeneous organic monolayers on metal surfaces. There have been numerous attempts to form well-ordered organic monolayers[1] by employing intermolecular covalent bonding,[2] hydrogen bonding,[3] electrostatic interactions,[4] and van der Waals interactions.[5] Metal–ligand networks, which use metal adatoms for binding molecules, are also useful to form well-ordered assemblies spontaneously. Chemical modification of molecules with functional groups that can serve as ligands such as cyanide, isocyanide, carboxylate, and pyridine, lead to substantial interaction with metal adatoms to form both two-dimensional (2D) networks and one-dimensional (1D) chains on metal substrates.[6] Although rigid frameworks can be constructed by this method,[7] the strong chemical bonding between metal and ligand that forms an organometallic complex may give rise to a significant change in intrinsic functional properties of the molecule. One potential strategy to simultaneously achieve the preservation of desired molecular properties and the fabrication of a stable molecular superstructure is conceived to use weak ion–dipole interactions, which are yet stronger than dipole–dipole and van der Waals interactions.

Diarylethene (DAE; the more specific term dithienylethene (DTE) is also used in some studies) could be one of the candidates to achieve supramolecular assembly through ion–dipole interactions, because it has an intrinsic dipole resulting from its unique structure (Scheme 1) and has no functional groups acting as a ligand with metal ions. DAE is well-known for its photochromism,[8] and thus switching properties as well as optoelectronic[9] and optomechanical[10] applications have been intensively studied.

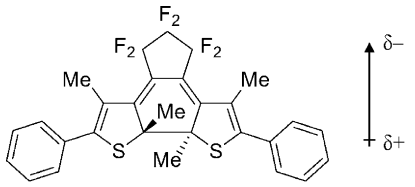


***Scheme 1.*** Structure of DAE molecule used in this study and the orientation of the molecular dipole moment. Calculated molecular dipole moment of the isolated molecule is 5.83 D.

Homogeneous monolayers composed of DAE have so far been achieved by designing and synthesizing modified DAE molecules: thiolated DAE for self-assembled monolayers (SAM) on Au(111)[11] and DAE with long alkyl chain and pyrene moieties, which is stabilized into a 2D structure at the solution/HOPG interface.[12] However, in these systems the strong intermolecular coupling may hamper control of the switching state of individual molecules.

Here, we report the successful formation of a metal ion–DAE superstructure using a simple DAE molecule called 1,2-bis(2,4-dimethyl-5-phenyl-3-thienyl)-3,3,4,4,5,5-hexafluoro-1-cyclopentene (see Figure 3 a for its gas phase structure) on the Cu(111) surface by co-deposition of NaCl followed by mild annealing. Based on scanning tunneling microscopy (STM) experiments and density functional theory (DFT) calculations, we propose a possible model for the superstructure, which consists of $Na^+$ ions and closed-form isomers of DAE. The driving force for the superstructure formation is indeed suggested to be ion–dipole interactions between $Na^+$ ions and the DAE molecules, which results in a row-type molecular arrangement along the molecular dipole axis.

Deposition of the closed-form isomer of DAE on the Cu(111) surface with pre-adsorbed NaCl islands under ultra-

[*] Dr. T. K. Shimizu,[+] Dr. J. Jung,[+] Dr. H. Imada, Dr. Y. Kim
Surface and Interface Science Laboratory, RIKEN
2-1 Hirosawa, Wako, Saitama 351-0198 (Japan)
E-mail: ykim@riken.jp
Homepage: http://www.riken.jp/Kimlab
Dr. T. K. Shimizu[+]
National Institute for Materials Science
1-2-1 Sengen, Tsukuba, Ibaraki 305-0047 (Japan)
[+] These authors contributed equally to this work.

[**] This work was supported by MEXT KAKENHI (grant number 21225001), JSPS KAKENHI (grant number 23760041), and the NIMS AF006 project. We thank E. Ito for technical assistance with XPS measurements. We are grateful for access to the RIKEN Integrated Cluster of Clusters (RICC) supercomputer system. J. Jung acknowledges the Foreign Postdoctoral Researcher (FPR) program of RIKEN for financial support.

Supporting information for this article is available on the WWW under http://dx.doi.org/10.1002/anie.201407555.

  

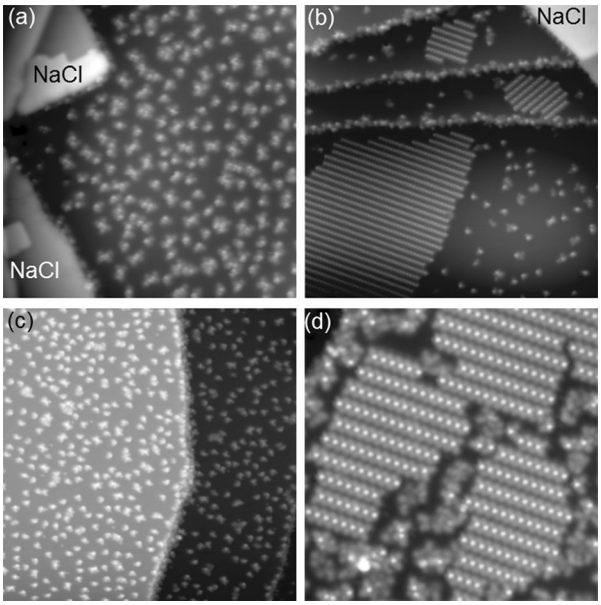


***Figure 1.*** STM images of closed-form DAE adsorbed on Cu(111) at room temperature with predeposited NaCl islands (indicated in the image), a) before and b) after annealing at 85 °C. c) Closed-form isomers adsorbed on clean Cu(111) at room temperature followed by annealing at 87 °C. d) DAE superstructure prepared by deposition of the closed-form isomer followed by deposition of NaCl and annealing at 85 °C. Image sizes: a) $50\times50$ nm$^2$, b,c) $80\times80$ nm$^2$, and d) $30\times30$ nm$^2$. Tunneling conditions: a,b) $V_s=-2$ V and $I_t=50$ pA, c) $V_s=+2$ V and $I_t=100$ pA, d) $V_s=+1$ V and $I_t=30$ pA.

high vacuum leads to a random distribution of adsorbed molecules on Cu(111), as shown in Figure 1a. All DAE molecules were found on clean Cu(111) regions and the rims of NaCl islands, and no molecules were adsorbed on the NaCl islands due to the smaller adsorption energy of DAE on top of the NaCl islands compared to that on Cu(111). After annealing the sample at ca. 360 K, well-ordered molecular films, which are composed of linear molecular rows, appeared on the Cu terraces, although some isolated DAE molecules were still present on the terraces and step edges of Cu, and the rims of the NaCl islands (Figure 1b). Three equivalent orientations of the row structure (two are shown in Figure 1b), along the $\langle 11\bar{2}\rangle$ directions of Cu(111), were found; these were identified by comparison with the orientation of the isolated molecules as well as with the crystal orientations clarified by the atomically resolved lattice of the Cu(111) surface.[13] The same superstructure was also formed by deposition of the open-form isomers, because the open-form isomer transforms into the closed-form isomer on Cu(111) using the thermal energy provided during annealing process. The stabilities of the two isomers are reversed on Cu(111) compared to that in solution.[13]

The co-deposition of NaCl is essential for the formation of a well-ordered DAE superstructure on Cu(111). Without NaCl, the molecules remained randomly adsorbed as isolated monomers, dimers, or small clusters even after annealing (Figure 1c). By postdepositing NaCl on the DAE/Cu(111) surface followed by annealing at about 360 K, we were able to fabricate molecular films (Figure 1d) that were identical to those formed by DAE deposition with preadsorbed NaCl islands (Figure 1b). These observations strongly indicate the necessity of Na, Cl, or both for superstructure formation.

Enlarged STM images are helpful for elucidating the details of the superstructure. All molecules are triangular with a bright spot at the center, and the DAE molecules within a molecular row adsorb in the identical structure with the same orientation; however, adjacent rows have opposite molecular orientations, as clarified by imaging the edges of the molecular film (Figure 2a) as well as the vacancies and voids within the films (Figure 2b). Small molecular clusters composed of two, three, and four DAE molecules on Cu(111) and Au(111) do not exhibit such a row-type adsorption configuration,[13] which also implies that the superstructure obtained by co-deposition of NaCl contains species other than DAE. Based on the STM contrast of the closed-form DAE and orientation of the Cu(111) lattice, we constructed a model of the superstructure, as displayed in Figure 2c. In this figure, the model is superimposed on an enlarged STM image taken from Figure 2b. The model uses the optimized structure of a single DAE row, which will be described in detail below. The basis vectors of the unit cell in the DAE superstructure, $u$ and

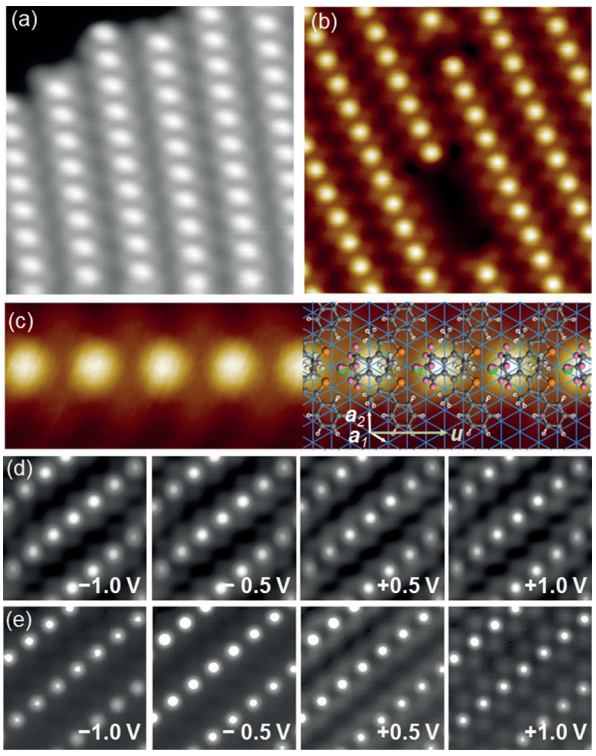


***Figure 2.*** a) STM image ($10\times10$ nm$^2$; $V_s=+1$ V and $I_t=30$ pA) of the edge region of the superstructure. b) STM image ($9\times9$ nm$^2$; $V_s=-1$ V and $I_t=30$ pA) of a DAE monolayer film containing a vacancy (one missing molecule) and void (four missing molecules). c) Proposed superstructure model superimposed on the enlarged, rotated, and trimmed STM image from (b). Unit vectors of the Cu(111) surface and one of the unit vectors of the superstructure are indicated. d) Bias dependence of the STM images ($5\times5$ nm$^2$) at $I_t=50$ pA. e) Constant height (feedback open at $V_s=+1$ V and $I_t=50$ pA) STS mappings ($5\times5$ nm$^2$). For (d) and (e), the sample bias is indicated in each image.

$v$, are defined as $u = 4a_1 + 2a_2$ and $v = 15a_2$, respectively, in which $a_1$ and $a_2$ are the unit vectors of the Cu(111) lattice. The bias dependences of the STM images (Figure 2d) and constant-height STS mapping (Figure 2e) are not significant within our experimental range of $\pm 2$ V. Only a small variation is found at the phenyl rings, which show brighter contrast in the unoccupied-state images ($V_s > 0$ V) than the occupied-state images ($V_s < 0$ V). We do not observe spots that could be attributed to $Na^+$ or $Cl^-$ ions.

Several groups have reported molecular superstructure formation through co-deposition of alkali halides. For molecular films of tetracyanoquinodimethane (TCNQ) on Au(111)[14] and terephthalic acid (TPA) on Cu(100)[7a] with NaCl co-deposition, the molecular packing geometries differ from those formed in the absence of alkali halides. Another report using biphenyl-3,3′,5,5′-tetracarboxylic acid (BTA) on Cu(100) showed that the molecule that does not form superstructures by itself does so when NaCl is co-deposited,[7b] which is quite similar to our case. In these previous reports, the observed superstructures were concluded to be molecule–alkali metal ionic crystals, and the disappearance of Cl was evidenced by the reduction of the Cl 2p peak during in situ X-ray photoelectron spectroscopy (XPS), in which the changes in the peak positions and intensities were recorded during or after molecular deposition on the metal with preadsorbed alkali halides. We also performed XPS experiments, but the two samples, i.e., NaCl/Cu(111) and DAE + NaCl/Cu(111), were prepared and measured in separate experiments; therefore, only the peak positions were compared. The results support the idea that Na binds to DAE and Cl disappears from the surface because of the penetration into the bulk, as proposed by Skomski et al.[7] (see the Supporting Information (SI) for details).

Although our case seems similar to previously reported molecule–alkali metal superstructures, there are significant differences. DAE does not possess any functional groups (such as carboxyl groups) that can act as ligands; thus, no chemical reaction with the metal ions to form ionic bonds is expected. Its low electron affinity ($EA$; $\approx 1.37$ eV[13]) does not predict the role of DAE as an electron acceptor to generate anions to form ionic crystals with positively charged alkali ions on Cu(111). In addition, the structures of the metal–molecule ionic crystals reported so far are two-dimensionally isotropic, whereas our case shows an anisotropic row structure. These differences indicate a unique bonding scheme that is distinguished from ionic bonding.

Periodic DFT calculations were carried out to gain insight into the formation of the DAE superstructure on Cu(111); we focused on the driving force leading to the anisotropic geometric configuration of the molecular film, i.e., the formation of a row structure (see SI for computation details). Therefore, we employed a supercell for an isolated single DAE molecular row, i.e., $b_1 = 4a_1 + 2a_2$ and $b_2 = 10a_2$, in which the smallest atomic distance between adjacent molecular rows was ca. 10 Å. We also investigated the role of the incorporated $Na^+$ ions in the formation of the molecular rows to explain our experimental findings, i.e., the successful fabrication of a DAE superstructure only with NaCl co-deposition. Extensive geometry optimizations were performed to obtain the most stable structure using the initial geometrical configurations of combinations of three adsorption orientations (i.e., P1, P2, and P3 according to the molecular plane facing the Cu(111) surface, as shown in Figure 3a) and four adsorption sites (on-top, OT; bridge, BR; fcc hollow site, *f*H; and hcp hollow site, *h*H according to the position of the center of mass of the DAE molecule).

Figure 3b and c show the most stable optimized structures for the molecular rows without and with $Na^+$ ions between neighboring DAE molecules, respectively (see Figures S2 and S3 for optimized structures of all the geometric configurations

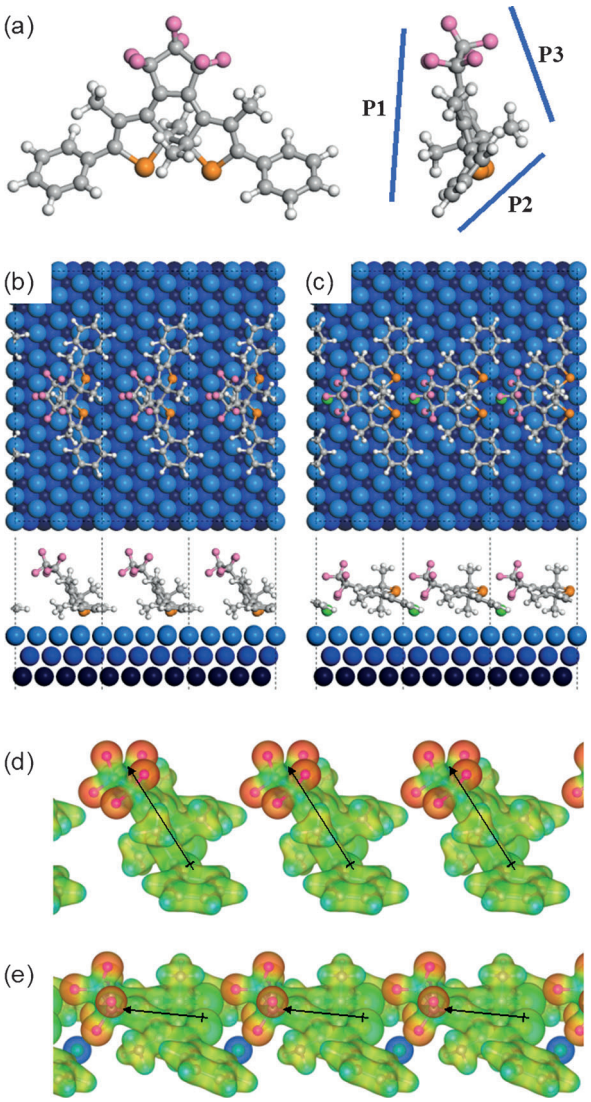


***Figure 3.*** a) Ball-stick model of closed-form DAE. On the right-hand side, a side view of the molecule and the three planes facing the Cu(111) surface considered in the calculations are shown; color code: gray C, white H, pink F, orange S. b) Top and side views of the DFT-optimized DAE row structure without $Na^+$. c) Top and side views of the DFT-optimized DAE row structure with $Na^+$ (green). d and e) Side views of the electrostatic potential maps of (b) and (c), respectively. Blue to red corresponds to positive to negative charges. Black arrows represent the molecular dipoles. Calculated molecular dipole moments on the Cu(111) surface for (d) and (e) are 10.11 D and 7.51 D, respectively.

considered in this study). In both cases, the hcp hollow site is the most stable adsorption site, although the relative energies of the optimized structures do not depend significantly on the adsorption site (see Table S1). Figure 3c displays a drastic change in adsorption geometry from that in Figure 3b because of the presence of $Na^+$ ions in the molecular row. Whereas the upright adsorption orientation (P2) of DAE molecules on Cu(111) is preferred in the absence of $Na^+$ ions (Figure 3b and S4), the flat-lying adsorption orientation (P1) is the most stable in the presence of $Na^+$ ions (Figures 3c and S5). In the absence of $Na^+$ ions, two sulfur atoms of the DAE molecule interact mainly with the Cu substrate; this is also accompanied by van der Waals interactions between the phenyl rings and the substrate (Figure S6). Thus, the DAE molecules should be oriented in the upright adsorption configuration. In contrast, when $Na^+$ ions are inserted between neighboring DAE molecules, the adsorption orientation in the molecular row is significantly altered, in which the $Na^+$ ions adsorbed on Cu(111) strongly interact with two fluorine atoms of DAE and thus draw the electronegative part of the DAE molecule closer to the substrate. Figure 3d and 3e show the electrostatic potential maps for isolated single DAE molecular rows without and with $Na^+$ ions, respectively, which clearly indicate that the attractive electrostatic interactions between $Na^+$ ions and DAE molecules modify the direction of the molecular dipole moment to be parallel to the substrate.

As a proof of ionization of the Na atoms on the Cu(111) surface, we show in Figure 4a and 4b the charge density difference maps for the molecular row without and with Na, respectively. Depletion of the charge around Na is clearly depicted (Figure 4b), and the net charge of Na is found to be $+0.77$ e. Ionization of Na is also confirmed in the density of states shown in Figure S7b, where Na 3s states are located in empty states away from the Fermi level. The ion–dipole interactions along the axis of the molecular row also compensate for the reduced interfacial interaction between the DAE molecules and the Cu(111) substrate. In the presence of Na, the charge transfer between the DAE molecule and the substrate is significantly reduced, and thus the charge density is redistributed, particularly around Na and F atoms (Figure 4b). The evaluated net molecular charges are $+0.51$ e and $-0.10$ e without and with $Na^+$ ions, respectively. The charge redistribution also leads to the decrease of molecular dipole moment (Figure 3) because electron depletion at S atoms and phenyl rings (green in Figure 4a) is recovered due to the geometric change. Accordingly, the change of the size and orientation of the molecular dipole moment as well as the ionization of Na results in a decrease of the work function by 0.37 eV with the surface coverage considered in our calculations. The reduction of substrate–molecule interactions is also indicated as sharpening of peaks in the density of states of the DAE molecules on Cu(111) (Figure S7). Therefore, our computational results strongly suggest that the ion–dipole interactions induced by $Na^+$ ions play a crucial role in the formation of an anisotropic geometric configuration, i.e., the formation of row structures along the axis of the ion–dipole interactions. The overall energy gain by Na incorporation along the molecular row in the superstructure, which is accompanied with charge redistribution, is found to be 0.64 eV ($E_{ad}$(DAE) = 4.32 eV; $E_{ad}$(DAE–Na) = 4.96 eV). STM image simulations of DAE rows without and with $Na^+$ ions also support our interpretation; experimental images agree well with the model with $Na^+$ ions (see SI for details.) The opposite directions of adjacent molecular rows may be related to geometrical preference to maximize the van der Waals interactions between adjacent molecules while maintaining the same adsorption sites, and antiparallel arrangement of the molecular dipoles, i.e., centrosymmetric arrangement, as is generally observed in molecular crystals.[15] In addition, because the reduction of the interfacial interactions might lead to changes in the path/rate of isomerization reactions, our results imply that co-deposition of atomic or ionic species would provide control of photochromism in a molecular film.

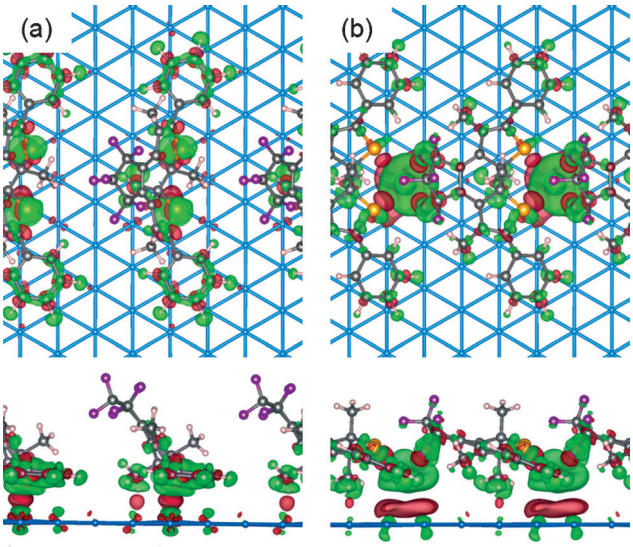


***Figure 4.*** Top and side views of the charge density difference maps for the DFT-optimized DAE row structures a) without and b) with $Na^+$. Red and green iso-surfaces indicate addition and depletion of electron density of $\pm 0.0012$ e bohr$^{-3}$, respectively. color code: gray C, white H, pink F, orange S, green Na.

In conclusion, we demonstrated the formation of a well-ordered superstructure of photochromic diarylethene molecules on Cu(111) by means of vacuum evaporation of either isomer with NaCl co-deposition followed by mild annealing. $Na^+$ incorporation is evident from a comparison of experimental STM images with DFT calculations. The key to the superstructure formation with anisotropic geometric configuration, i.e., the formation of a linear row structure, is suggested to be cation–molecular dipole interactions. Although further experiments to accomplish photochromic reactions within the superstructure are necessary, our results demonstrate a potential strategy to utilize alkali metal co-deposition to simultaneously control electronic properties and tune intermolecular interactions. Knowledge of the interactions involved could also be useful for designing new molecules for optoelectronic devices.

## Experimental Section

STM experiments were performed using a low-temperature STM system (Omicron GmbH) in an ultrahigh vacuum (UHV) chamber. The base pressure was less than $5 \times 10^{-11}$ Torr. All STM measurements were performed at 5 K. Constant height STS mappings were acquired using a standard lock-in technique with a bias modulation of 40 mV and 617 Hz while opening the feed-back loop. All bias voltages indicated in this Communication are with respect to the sample, i.e., $V_{sample}$.

Cu(111) was prepared by repeated cycles of $Ar^+$ ion sputtering and annealing. NaCl islands (2–3 monolayers thick) were formed at room temperature (RT) by evaporation from a Knudsen cell (K-cell) heated at 870–900 K. The molecule purchased was the open-form isomer of 1,2-bis(2,4-dimethyl-5-phenyl-3-thienyl)-3,3,4,4,5,5-hexafluoro-1-cyclopentene (98% purity, Tokyo Chemical Industry Co., Ltd.). The powder was degassed in the K-cell before deposition, and the temperature at the K-cell was at ≈400 K, and the Cu(111) substrate was kept at RT during deposition. When the closed-form isomer was used for deposition, the powder was exposed to UV light (375 nm) until it turned to blue prior to insertion into the K-cell. Cu(111) was annealed at 355–365 K to form the superstructure.

X-ray photoelectron spectroscopy (XPS) was performed in another UHV system that was equipped with a Theta Probe system (Thermo Fischer Scientific) with a monochromatized Al Kα X-ray source. The spectra were calibrated using the Cu 2p 3/2 peak at 932.4 eV. The prepared samples, i.e., NaCl/Cu(111) and DAE + NaCl/Cu(111), were transferred from the sample preparation chamber of the STM system to the XPS system using a portable UHV chamber.

Received: July 24, 2014
Revised: September 7, 2014
Published online: October 29, 2014

**Keywords:** density functional calculations · diarylethene · scanning probe microscopy · supramolecular chemistry

[1] a) L. Bartels, *Nat. Chem.* **2010**, *2*, 87 – 95; b) J. V. Barth, *Surf. Sci.* **2009**, *603*, 1533 – 1541.

[2] a) A. Gourdon, *Angew. Chem. Int. Ed.* **2008**, *47*, 6950 – 6953; *Angew. Chem.* **2008**, *120*, 7056 – 7059; b) L. Grill, M. Dyer, M. L. Lafferentz, M. Persson, M. V. Peters, S. Hecht, *Nat. Nanotechnol.* **2007**, *2*, 687 – 691.

[3] a) G. Pawin, K. L. Wong, K.-Y. Kwon, L. Bartels, *Science* **2006**, *313*, 961 – 962; b) J. A. Theobald, N. S. Oxtoby, M. A. Phillips, N. R. Champness, P. H. Beton, *Nature* **2003**, *424*, 1029 – 1031; c) W. Chen, H. Li, H. Huang, Y. Fu, H. L. Zhang, J. Ma, A. T. S. Wee, *J. Am. Chem. Soc.* **2008**, *130*, 12285 – 12289; d) U. Schlickum, R. Decker, F. Klappenberger, G. Zoppellaro, S. Klyatskaya, W. Auwärter, S. Neppl, K. Kern, H. Brune, M. Ruben, J. V. Barth, *J. Am. Chem. Soc.* **2008**, *130*, 11778 – 11782; e) J. V. Barth, J. Weckesser, C. Cai, P. Günter, L. Bürgi, O. Jeandupeux, K. Kern, *Angew. Chem. Int. Ed.* **2000**, *39*, 1230 – 1234; *Angew. Chem.* **2000**, *112*, 1285 – 1288; f) K. Ueji, J. Jung, J. Oh, K. Miyamura, Y. Kim, *Chem. Commun.* **2014**, *50*, 11230 – 11234.

[4] T. K. Shimizu, J. Jung, T. Otani, Y.-K. Han, M. Kawai, Y. Kim, *ACS Nano* **2012**, *6*, 2679 – 2685.

[5] a) C. Rogero, J. I. Pascual, J. Gómez-Herrero, A. M. Baró, *J. Chem. Phys.* **2002**, *116*, 832 – 836; b) J. K. Gimzewski, S. Modesti, T. David, R. R. Schlittler, *J. Vac. Sci. Technol. B* **1994**, *12*, 1942 – 1946; c) J.-H. Kim, K. Tahara, J. Jung, S. De Feyter, Y. Tobe, Y. Kim, M. Kawai, *J. Phys. Chem. C* **2012**, *116*, 17082 – 17088.

[6] a) U. Schlickum, R. Decker, F. Klappenberger, G. Zoppellaro, S. Klyatskaya, M. Ruben, I. Silanes, A. Arnau, K. Kern, H. Brune, J. V. Barth, *Nano Lett.* **2007**, *7*, 3813 – 3817; b) A. Dmitriev, H. Spillmann, N. Lin, J. V. Barth, K. Kern, *Angew. Chem. Int. Ed.* **2003**, *42*, 2670 – 2673; *Angew. Chem.* **2003**, *115*, 2774 – 2777; c) S. Stepanow, M. Lingefelder, A. Dmitriev, H. Spillmann, E. Delvigne, N. Lin, X. Deng, C. Cai, J. V. Barth, K. Kern, *Nat. Mater.* **2004**, *3*, 229 – 233; d) M. N. Faraggi, N. Jiang, N. Gonzalez-Lakunza, A. Langner, S. Stepanow, K. Kern, A. Arnau, *J. Phys. Chem. C* **2012**, *116*, 24558 – 24565; e) A. Breitruck, H. E. Hoster, R. J. Behm, *J. Phys. Chem. C* **2009**, *113*, 21265 – 21268; f) T. Classen, G. Fratesi, G. Costantini, S. Fabris, F. L. Stadler, C. Kim, S. de Gironcoli, S. Baroni, K. Kern, *Angew. Chem. Int. Ed.* **2005**, *44*, 6142 – 6145; *Angew. Chem.* **2005**, *117*, 6298 – 6301; g) S. L. Tait, A. Langner, N. Lin, S. Stepanow, Ch. Rajadurai, M. Ruben, K. Kern, *J. Phys. Chem. C* **2007**, *111*, 10982 – 10987.

[7] a) D. Skomski, S. Abb, S. L. Tait, *J. Am. Chem. Soc.* **2012**, *134*, 14165 – 14171; b) D. Skomski, S. L. Tait, *J. Phys. Chem. C* **2013**, *117*, 2959 – 2965.

[8] a) M. Irie, *Proc. Jpn. Acad. Ser. B* **2010**, *86*, 472 – 483; b) S. Kobatake, M. Irie, *Bull. Chem. Soc. Jpn.* **2004**, *77*, 195 – 210; c) M. Irie, S. Kobatake, M. Horichi, *Science* **2001**, *291*, 1769 – 1772; d) M. Irie, *Chem. Rev.* **2000**, *100*, 1685 – 1716.

[9] a) R. C. Shallcross, P. Zacharias, A. Köhnen, P. O. Körner, E. Maibach, K. Meerholz, *Adv. Mater.* **2013**, *25*, 469 – 476; b) R. Hayakawa, K. Higashiguchi, K. Matsuda, T. Chikyow, Y. Wakayama, *ACS Appl. Mater. Interfaces* **2013**, *5*, 3625 – 3630; c) T. Tsujioka, T. Sasa, Y. Kakihara, *Org. Electron.* **2012**, *13*, 681 – 686.

[10] a) F. Terao, M. Morimoto, M. Irie, *Angew. Chem. Int. Ed.* **2012**, *51*, 901 – 904; *Angew. Chem.* **2012**, *124*, 925 – 928; b) M. Morimoto, M. Irie, *J. Am. Chem. Soc.* **2010**, *132*, 14172 – 14178.

[11] a) S. V. Snegir, A. A. Marchenko, P. Yu, F. Maurel, O. L. Kapitanchuk, S. Mazerat, M. Lepeltier, A. Léaustic, E. Lacaze, *J. Phys. Chem. Lett.* **2011**, *2*, 2433 – 2436; b) N. Katsonis, T. Kudernac, M. Walko, S. J. van der Molen, B. J. van Wees, B. L. Feringa, *Adv. Mater.* **2006**, *18*, 1397 – 1400.

[12] R. Arai, S. Uemura, M. Irie, K. Matsuda, *J. Am. Chem. Soc.* **2008**, *130*, 9371 – 9379.

[13] T. K. Shimizu, J. Jung, H. Imada, Y. Kim, *Chem. Commun.* **2013**, *49*, 8710 – 8712.

[14] C. Wäckerlin, C. Iacovita, D. Chylarecka, P. Fesser, T. A. Jung, N. Ballav, *Chem. Commun.* **2011**, *47*, 9146 – 9148.

[15] S. Kimura, *Org. Biomol. Chem.* **2008**, *6*, 1143 – 1148.

  